発表者氏名	論文タイトル名	発表誌名	巻名	ページ	出版年
Ogura M, Hatake K, Ando K, Tobinai K, Tokushige K, Ono C, Ishibashi T, Vandendries E.	Phase I Study of Anti-CD22 Immunoconjugate Inotuzumab Ozogamicin Plus Rituximab in Relapsed/Refractory B-cell Non-Hodgkin Lymphoma.	Cancer Science,	103	933-938,	2012
Matsushita H, Nakamura N, Tanaka Y, Ohgiya D, Tanaka Y, Damdinsuren A, Ogawa Y, Ando K, Miyachi H.	Clinical and pathological features of B-cell non-Hodgkin lymphomas lacking surface expression of immunoglobulin light chains.	Clinical Chemistry and Laboratory Medicine,	50	1665-1670	2012
Shirasugi Y, Ando K, Miyazaki K, Tomiyama Y, Iwato K, Okamoto S, Kurokawa M, Kirito K, Hashino S, Ninomiya H, Mori S, Yonemura Y, Usuki K, Wei H, Lizambri R.	An Open-Label Extension Study Evaluating the Safety and Efficacy of up to 3.5 years of Romiplostim in Thrombocytopenic Japanese Patients with Immune Thrombocytopenic Purpura (ITP)	Int J Hematol	95	,652-659	2012
Eren M, Boe AE, Murphy SB, Place AT, Nagpal V, Morales-Nebreda L, Urich D, Quaggin SE, Budinger GS, Mutlu GM, Miyata T, Vaughan DE.	PAI-1-regulated extracellular proteolysis governs senescence and survival in Klotho mice	Proc Natl Acad Sci USA	111	7090-7095.	2014
Ibrahim AA, Yahata T, Onizuka M, Dan T, van Ypersele de Strihou C, Miyata T, Ando K.	Inhibition of Plasminogen Activator Inhibitor Type-1 Activity Enhances Rapid and Sustainable Hematopoietic Regeneration	Stem Cells	32	946-58	2014
Kobayashi N, Ueno T, Ohashi K, Yamashita H, Takahashi Y, Sakamoto K, Manabe S, Hara S, Takashima Y, Dan T, Pastan I, Miyata T, Kurihara H, Matsusaka T, Reiser J, Nagata M.	Podocyte injury-driven intracapillary plasminogen activator inhibitor type 1 accelerates podocyte loss via beta 1 integrin endocytosis	Am J Physiol Renal Physiol	308	F614-26	2015
Boe AE, Eren M, Morales-Nebreda L, Murphy SB, Budinger GR, Mutlu GM, Miyata T, Vaughan DE.	Nitric oxide prevents alveolar senescence and emphysema in a mouse model.	PLoS One	10	e0116504	2015
Nicolas Pelisch , Takashi Dan , Atsuhiko Ichimura , Hiroki Sekiguchi , Douglas E. Vaughan , Charles van Ypersele de Strihou , and Toshio Miyata	Plasminogen Activator Inhibitor-1 Antagonist TM5484 Attenuates Demyelination and Axonal Degeneration	PLoS One	pr 27; 10(4)	e0124510. doi: 10.1371/journal.pone.0124510..	2015
Remuzzi G1, Benigni A, Finkelstein FO, Grunfeld JP, Joly D, Katz I, Liu ZH, Miyata T, Perico N, Rodriguez-Iturbe B, Antiga L, Schaefer F, Schieppati A, Schrier RW, Tonelli M.	Kidney failure: aims for the next 10 years and barriers to success.	Lancet	27;382 (9889)	353-62	2013
Huang WT, Vayalil PK, Miyata T, Hagood J, Liu RM.	Therapeutic value of small molecule inhibitor to plasminogen activator inhibitor-1 for lung fibrosis.	Am J Respir Cell Mol Biol	46	87-95	2012

発表者氏名	論文タイトル名	発表誌名	巻名	ページ	出版年
Dan T, Yamaki S, Sato Y, Kiyomoto H, Ishii N, Okada K, Matsuo O, Hou FF, Vaughan DE, van Ypersele de Strihou C, Miyata T.	A Small Molecule Inhibitor to Plasminogen Activator Inhibitor 1 Inhibits Macrophage Migration.	Arterioscler Thromb Vasc Biol.	33(5):9	35-42	2013
Lai CY, Yamazaki S, Okabe M, Suzuki S, Maeyama Y, Iimura Y, Onodera M, Kakuta S, Iwakura Y, Nojima M, Otsu M, Nakauchi H.	Stage-specific roles for CXCR4 signaling in murine hematopoietic stem/progenitor cells in the process of bone marrow repopulation.	Stem Cells	32(7)	1929-42	2014
Matsunawa M, Yamamoto R, Sanada M, Sato-Otsubo A, Shiozawa Y, Yoshida K, Otsu M, Shiraishi Y, Miyano S, Isono K, Koseki H, Nakauchi H, Ogawa S. Leukemia.	Haploinsufficiency of Sf3b1 leads to compromised stem cell function but not to myelodysplasia.	Leukemia	28(9)	1844-50	2014
Nakahara F, Kitaura J, Uchida T, Nishida C, Togami K, Inoue D, Matsukawa T, Kagiyama Y, Enomoto Y, Kawabata KC, Lai CY, Komeno Y, Izawa K, Oki T, Nagae G, Harada Y, Harada H, Otsu M, Aburatani H, Heissig B, Hattori K, Kitamura T.	Hes1 promotes blast crisis in chronic myelogenous leukemia through MMP-9 upregulation in leukemic cells.	Blood	123(25)	3932-42	2014
Suzuki N, Yamazaki S, Yamaguchi T, Okabe M, Masaki H, Takaki S, Otsu M, Nakauchi H.	Generation of engraftable hematopoietic stem cells from induced pluripotent stem cells by way of teratoma formation.	Mol Ther	21(7)	1424-31	2013
Saka K, Kawahara M, Teng J, Otsu M, Nakauchi H, Nagamune T	Top-down motif engineering of a cytokine receptor for directing ex vivo expansion of hematopoietic stem cells.	J Biotechnol	168(4)	659-65	2013
Kon A, Shih LY, Minamino M, Sanada M, Shiraishi Y, Nagata Y, Yoshida K, Okuno Y, Bando M, Nakato R, Ishikawa S, Sato-Otsubo A, Nagae G, Nishimoto A, Haferlach C, Nowak D, Sato Y, Alpermann T, Nagasaki M, Shimamura T, Tanaka H, Chiba K, Yamamoto R, Yamaguchi T, Otsu M, Obara N, Sakata-Yanagimoto M, Nakamaki T, Ishiyama K, Nolte F, Hofmann WK, Miyawaki S, Chiba S, Mori H, Nakauchi H, Koeffler HP, Aburatani H, Haferlach T, Shirahige K, Miyano S, Ogawa S.	Recurrent mutations in multiple components of the cohesin complex in myeloid neoplasms.	Nat Genet	45(10)	1232-7	2013

発表者氏名	論文タイトル名	発表誌名	巻名	ページ	出版年
Lin HT, Otsu M, Nakauchi H.	Stem cell therapy: an exercise in patience and prudence.	Philosophical transactions of the Royal Society of London Series B, Biological sciences.	368	1609	2013
Nishimura S, Manabe I, Nagasaki M, Kakuta S, Iwakura Y, Takayama N, Ooehara J, Otsu M, Kamiya A, Petrich BG, Urano T, Kadono T, Sato S, Aiba A, Yamashita H, Sugiura S, Kadowaki T, Nakauchi H, Eto K, Nagai R.	In vivo imaging visualizes discoid platelet aggregations without endothelium disruption and implicates contribution of inflammatory cytokine and integrin signaling.	Blood	119 (8)	e45-56	2012
Nakanishi M and Otsu M.	Development of Sendai Virus Vectors and Their Potential Applications in Gene Therapy and Regenerative Medicine.	Current gene therapy	12 (5)	410-416	2012
Wang C, Sashida G, Saraya A, Ishiga R, Koide S, Oshima M, Ishono K, Koseki H, and Iwama A.	Depletion of Sf3b1 impairs proliferative capacity of hematopoietic stem cells but is not sufficient to induce myelodysplasia.	Blood	123	3336-3343	2014
Sashida G, Harada H, Matsui H, Oshima M, Yui M, Harada Y, Tanaka S, Mochizuki-Kashio M, Wang C, Saraya A, Muto T, Inaba T, Koseki H, Huang G, Kitamura T, and Iwama A.	Ezh2 loss promotes development of myelodysplastic syndrome but attenuates its predisposition to leukemic transformation.	Nat Commun	5	4177	2014
Miyagi S, Koide S, Saraya A, Wendt GR, Oshima M, Konuma T, Yamazaki S, Mochizuki-Kashio M, Nakajima-Takagi Y, Wang C, Chiba T, Kitabayashi I, Nakauchi H and Iwama A.	The Tif1β-Hp1 system maintains transcriptional integrity of hematopoietic stem cells.	Stem Cell Reports	2	145-152	2014
Nakajima-Takagi Y, Osawa M, and Iwama A.	Manipulation of hematopoietic stem cells for regenerative medicine.	Anat Rec	297	111-120	2014
Muto T, Sashida G, Oshima M, Wendt GR, Mochizuki-Kashio M, Nagata Y, Sanada M, Miyagi S, Saraya A, Kamio A, Nagae G, Nakaseko C, Yokote K, Shimoda K, Koseki H, Suzuki Y, Sugano S, Aburatani H, Ogawa S, and Iwama A.	Concurrent loss of Ezh2 and Tet2 cooperates in the pathogenesis of myelodysplastic disorders.	J Exp Med	210	2627-2639	2013

発表者氏名	論文タイトル名	発表誌名	巻名	ページ	出版年
Nishino T, Osawa M, and Iwama A.	New approaches to expand hematopoietic stem and progenitor cells.	Expert Opin Biol Ther	12	743-756	2012
Nakamura S, Oshima M, Yuan J, Saraya A, Miyagi S, Konuma T, Yamazaki S, Osawa M, Nakauchi H, Koseki H, and Iwama A.	Bmi1 confers resistance to oxidative stress on hematopoietic stem cells.	PLoS ONE	7	e36209,	2012
Nakajima-Takagi Y, Osawa M, Oshima M, Takagi H, Miyagi S, Endoh M, Endo TA, Takayama N, Eto K, Toyoda T, Koseki H, Nakauchi H, and Iwama A.	Role of SOX17 in hematopoietic development from human embryonic stem cells.	Blood	121	447-458	2013
Koura U, Sakaki-Nakatsubo H, Otsubo K, Nomura K, Oshima K, Ohara O, Wada T, Yachie A, Imai K, Morio T, Miyawaki T, Kanegane H.	Successful treatment of systemic cytomegalovirus infection in severe combined immunodeficiency using allogeneic bone marrow transplantation followed by adoptive immunotherapy.	J Investig Allergol Clin Immunol.	24(3)	200-2.	2014
Endo A, Watanabe K, Ohye T, Suzuki K, Matsubara T, Shimizu N, Kurahashi H, Yoshikawa T, Katano H6, Inoue N, Imai K, Takagi M, Morio T, Mizutani 8.	Molecular and virological evidence of viral activation from chromosomally integrated human herpesvirus 6A in a patient with X-linked severe combined immunodeficiency.	Clin Infect Dis.	59(4)	545-8.	2014
Nakatani K, Imai K, Shigeno M, Sato H, Tezuka M, Okawa T, Mitsuiki N1, Isoda T, Tomizawa D, Takagi M, Nagasawa M, Kajiwara M, Yamamoto M, Arai A, Miura O, Kamae C, Nakagawa N, Honma K, Nonoyama S, Mizutani S, Morio T.	Cord blood transplantation is associated with rapid B-cell neogenesis compared with BM transplantation.	Bone Marrow Transplant.	49(9)	1155-61.	2014
Kumaki S, Sasahara Y, Kamachi Y, Muramatsu H, **Morio T**, Goi K, Sugita K, Urabe T, Takada H, Kojima S, Tsuchiya S, Hara T.	B-cell function after unrelated umbilical cord blood transplantation using a minimal-intensity conditioning regimen in patients with X-SCID.	Int J Hematol.	98	355-60,	2013
森尾友宏、宮坂あかね、小野敏明、落合　央、藤田由利子、高橋　聡	移植後ウイルス感染に対する多ウイルス特異的CTL療法	The Japanese Journal of Pediatric Hematology Oncology	50(3)	335-340	2013
Munakata S, Tashiro Y, Nishida C, Sato A, Komiyama H, Shimazu H, Dhahri D, Salama Y, Eiamboonsert S, Takeda K, Yagita H, Tsuda Y, Okada Y, Nakauchi H, Sakamoto K, Heissig B, Hattori K	Inhibition of Plaamin Protects Agents Colitis in Mice by SuppressingMatrix Metalloproteinase 9-mediated Cytokine Release from Myeloid Cells.	Gastroenterology	48(3)	565-578	2015

発表者氏名	論文タイトル名	発表誌名	巻名	ページ	出版年
Sato A, Nishida C, Sato-Kusubata K, Ishihara M, Tashiro Y, Gritli I, Shimazu H, Munakata S, Yagita H, Okumura K, Tsuda Y, Okada Y, Tojo A, Nakauchi H, Takahashi S, Heissig B and Hattori K.	Inhibition of plasmin attenuates murine acute graft-versus-host disease mortality by suppressing the matrix metalloproteinase-9-dependent inflammatory cytokine storm and effector cell trafficking.	Leukemia	29(1)	145-56.	2015
Fumio Nakahara, Jiro Kitaura, Tomoyuki Uchida, Chiemi Nishida, Katsuhiro Togami,Daichi Inoue Toshihiro Matsukawa,Yuki Kagiyama, Yutaka Enomoto, Kimihito C. Kawabata, Lai Chen-Yi, Yukiko Komeno, Kumi Izawa, Toshihiko Oki,Genta Nagae,5 Yuka Harada, Hironori Harada, Makoto Otsu, Hiroyuki Aburatani, Beate Heissig, Koichi Hattori, and Toshio Kitamura,	Hes1 promotes blast crisis in chronic myelogenous leukemia through MMP-9 upregulation in leukemic cells	Blood	19;123(25)	3932-42.	2014
Nishida C, Kusubata K, Tashiro Y, Gritli I, Sato A, Ohki-Koizumi M, Morita Y, Nagano M, Sakamoto T, Koshikawa N, Kuchimaru T, Kizaka-Kondoh S, Seiki M, Nakauchi H, Heissig B, and Hattori K	MT1-MMP plays a critical role in hematopoiesis by regulating HIF-mediated chemo-/cytokine gene transcription within niche cells.	Blood	119 (23)	5405-5416	2012
Tashiro Y, Nishida C, Sato-Kusubata K, Ohki-Koizumi M, Ishihara M, Sato A, Gritli I, Komiyama H, Sato Y, Tomiki Y, Sakamoto H, Dan T, Miyata T, Okumura K, Nakauchi H, Heissig B, and Hattori K	Inhibition of PAI-1 induces neutrophil-driven neoangiogenesis and promotes tissue regeneration via production of angiocrine factors in mice	Blood	119 (26)	6382-6393	2012
Ishihara M, Nishida C, Tashiro Y, Gritli I, Rosenkvist J, Koizumi M, Yamamoto R, Yagita H, Okumura K, Nishikori M, Wanaka K, Tsuda Y, Okada Y, Nakauchi H, Heissig B, Hattori K	Plasmin inhibitor reduces T-cell lymphoid tumor growth by suppressing matrix metalloproteinase-9-dependent CD11b+/F4/80+ myeloid cell recruitment	Leukemia	26	332-339	2012
Caiado F, Carvalho T, Rosa I, Remedio L, Costa A, Matos J, Heissig B, Yagita H, Hattori K, da Silva JP, Fidalgo P, Dias Pereira A, Dias S	Bone marrow-derived CD11b+Jagged-2+ cells promote epithelial to mesenchymal transition and metastization in colorectal cancer	Cancer Res	73 (14)	4233-46	2013
Kanda Y, Kanda J, Atsuta Y, Fuji S, Maeda Y, Ichinohe T, Takanashi M, Ohashi K, Fukuda T, Miyamura K, Mori T, Sao H, Kobayashi N, Iwato K, Sawada A, Mori S; HLA working group of the Japan Society for Hematopoietic Cell Transplantation.	Changes in the Clinical Impact of High-Risk Human Leukocyte Antigen Allele Mismatch Combinations on the Outcome of Unrelated Bone Marrow Transplantation.	Biol Blood Marrow Transplant.	20(4):	526-35.	2014

発表者氏名	論文タイトル名	発表誌名	巻名	ページ	出版年
Abe T, Shimada E, Takanashi M, Takamura T, Motoji K, Okazaki H, Satake M, Tadokoro K.	Antibody against immunoglobulin E contained in blood components as causative factor for anaphylactic transfusion reactions.	Transfusion	54(8)	1953-60	2014
Pamphilon D, Selogie E, McKenna D, Cancelas-Peres JA, Szczepiorkowski ZM, Sacher R, McMannis J, Eichler H, Garritsen H, Takanashi M, van de Watering L, Stroncek D, Reems JA.	Current practices and prospects for standardization of the hematopoietic colony-forming unit assay: a report by the cellular therapy team of the Biomedical Excellence for Safer Transfusion (BEST) Collaborative	Cytotherapy	15(3)	255-262	2013
Yamaguchi R, Takanashi M, Ito M, Ogawa A, Hashimoto M, Ishii Y, Mazda T, Tadokoro K, Nakajima K, Minami M.	Plasticizer concentration in cord blood cryopreserved with DMSO.	Bone Marrow Transplant	49(1)	157-8	2014
van der Meer PF, Reesink HW, Panzer S, Wong J, Ismay S, Keller A, Pink J, Buchta C, Compernolle V, Wendel S, Biagini S, Scuracchio P, Thibault L, Germain M, Georgsen J, Bégué S, Dernis D, Raspollini E, Villa S, Rebulla P, Takanashi M, de Korte D, Lozano M, Cid J, Gulliksson H, Cardigan R, Tooke C, Fung MK, Luban NL, Vassallo R, Benjamin R.	Should DEHP be eliminated in blood bags?	Vox Sang.	106(2)	176-195	2014
Eichler H, Schrezenmeier H, Schallmoser K, Strunk D, Nystedt J, Kaartinen T, Korhonen M, Fleury-Cappellesso S, Sensebé L, Bönig H, Rebulla P, Giordano R, Lecchi L, Takanashi M, Watt SM, Austin EB, Guttridge M, McLaughlin LS, Panzer S, Reesink HW.	Donor selection and release criteria of cellular therapy products.	Vox Sanguinis	104(1)	67-91	2013
Takanashi M, Odajima T, Aota S, Sudoh M, Yamaga Y, Ono Y, Yoshinaga K, Motoji T, Matsuzaki K, Satake M, Sugimori H, Nakajima K.	Risk factor analysis of vasovagal reaction from blood donation.	Transfus Apher Sci.	47(3)	319-325	2012
Kanda J, Hishizawa M, Utsunomiya A, Taniguchi S, Eto T, Moriuchi Y, Tanosaki R, Kawano F, Miyazaki Y, Masuda M, Nagafuji K, Hara M, Takanashi M, Kai S, Atsuta Y, Suzuki R, Kawase T, Matsuo K, Nagamura-Inoue T, Kato S, Sakamaki H, Morishima Y, Okamura J, Ichinohe T, Uchiyama T.	Impact of graft-versus-host disease on outcomes after allogeneic hematopoietic cell transplantation for adult T-cell leukemia: a retrospective cohort study.	Blood	119(9)	2141-8	2012

発表者氏名	論文タイトル名	発表誌名	巻名	ページ	出版年
Kanda J, Nakasone H, Atsuta Y, Toubai T, Yokoyama H, Fukuda T, Taniguchi S, Ohashi K, Ogawa H, Eto T, Miyamura K, Morishima Y, Nagamura-Inoue T, Sakamaki H, Murata M.	Risk factors and organ involvement of chronic GVHD in Japan.	Bone Marrow Transplant.	,Feb;49(2):.	228-35, doi: 10.1038/bmt.2013.151. Epub 2013 Sep 30	2014
Imahashi N, Imamoto T, Ito M, Koyama D, Goto T, Onodera K, Seto A, Watanabe K, Imahashi M, Nishiwaki S, Tsukamoto S, Yasuda T, Ozawa Y, Miyamura K.	Clinical significance of hemophagocytos is in BM clot sections during the peri-engraftment period following allogeneic hematopoietic SCT.	Bone Marrow Transplant	47	387－94	2012
Kanda J, Saji H, Fukuda T, Kobayashi T, Miyamura K, Eto T, Kurokawa M, Kanamori H, Mori T, Hidaka M, Iwato K, Yoshida T, Sakamaki H, Tanaka J, Kawa K, Morishima Y, Suzuki R, Atsuta Y, Kanda Y.	Related transplantation with HLA-1 Ag mismatch in the GVH direction and HLA-8/8 allele-matched unrelated transplantation: a nationwide retrospective study.	Blood	119	2409-16	2012
Nishiwaki S, Miyamura K, Ohashi K, Kurokawa M, Taniguchi S, Fukuda T, Ikegame K, Takahashi S, Mori T, Imai K, Iida H, Hidaka M, Sakamaki H, Morishima Y, Kato K, Suzuki R, Tanaka J; for the Adult Acute Lymphoblastic Leukemia Working Group of the Japan Society for Hematopoietic Cell Transplantation.	Impact of a donor source on adult Philadelphia chromosome-negative acute lymphoblastic leukemia: a retrospective analysis from the Adult Acute Lymphoblastic Leukemia Working Group of the Japan Society for Hematopoietic Cell Transplantation.	Ann Oncol	24	1595-1602	2012
Imahashi N, Ohashi H, Terakura S, Miyao K, Sakemura R, Kato T, Sawa M, Yokohata E, Kurahashi S, Ozawa Y, Nishida T, Kiyoi H, Watamoto K, Kohno A, Kasai M, Kato C, Iida H, Naoe T, Miyamura K, Murata M; for the Nagoya Blood and Marrow Transplantation Group.	Chimerism status after unrelated donor bone marrow transplantation with fludarabine-melphalan conditioning is affected by the melphalan dose and is predictive of relapse.	Ann Hematol	Epub ahead of print	PMID: 25680895	2015
Tanaka M, Miyamura K, Terakura S, Imai K, Uchida N, Ago H, Sakura T, Eto T, Ohashi K, Fukuda T, Taniguchi S, Mori S, Nagamura-Inoue T, Atsuta Y, Okamoto S.	Comparison of Cord Blood Transplantation with Unrelated Bone Marrow Transplantation in Patients Older than Fifty Years.	Biol Blood Marrow Transplant.	21(3)	517-25.	2014
Terakura S, Nishida T, Inamoto Y, Ohashi H, Naoe T, Murata M.	Successful unrelated cord blood transplantation for adult acquired aplastic anemia using reduced intensity conditioning without ATG.	Immunol Lett.	160(1)	99-101.	2014
Matsuno N, Yamamoto H, Watanabe N, Uchida N, Ota H, Nishida A, Ikebe T, Ishiwata K, Nakano N, Tsuji M, Asano-Mori Y, Izutsu K, Masuoka K, Wake A, Yoneyama A, Nakauchi H, Taniguchi S.	Rapid T-cell chimerism switch and memory T-cell expansion are associated with pre-engraftment immune reaction early after cord blood transplantation	Br J Haematol	160(2)	255-8	2013

発表者氏名	論文タイトル名	発表誌名	巻名	ページ	出版年
Hisashi Yamamoto, Naoyuki Uchida, Naofumi Matsuno, Hikari Ota, Kosei Kageyama, Sachie Wada, Daisuke Kaji, Aya Nishida, Kazuya Ishiwata, Shinsuke Takagi, Masanori Tsuji, Yuki Asano-Mori, Go Yamamoto, Koji Izutsu, Kazuhiro Masuoka, Atsushi Wake, Akiko Yoneyama, Shigeyoshi Makino, Shuichi Taniguchi.	Anti-HLA Antibodies Other than Against HLA-A, -B, -DRB1 Adversely Affect Engraftment and Nonrelapse Mortality in HLA-Mismatched Single Cord Blood Transplantation: Possible Implications of Unrecognized Donor-specific Antibodies.	Biol Blood Marrow Transplant.	20(10)	1634-1640	2014
H Yamamoto, N Uchida, N Matsuno, A Kon, A Nishida,H Ota, T Ikebe, N Nakano, K Ishiwata, H Araoka, S Takagi, M Tsuji, Y Asano-Mori, G Yamamoto, K Izutsu, K Masuoka, A Wake, A Yoneyama, S Makino and S Taniguchi.	I.v. BU/fludarabine plus melphalan or TBI in unrelated cord blood transplantation for high-risk hematological diseases.	Bone Marrow Transplantation.	advance online publication,	40568	2015
Mori J, Ohashi K, Yamaguchi T, Ando M, Hirashima Y, Kobayashi T, Kakihana K, Sakamaki H.	Risk assessment for acute kidney injury after allogeneic hematopoietic stem cell transplantation based on acute kidney injury network criteria.	Internal Medicine,	51(16)	:2105-10,	2012

Ⅳ．研究成果の刊行物・別刷

（主なもの）

Leukemia (2015) **29,** 145–156
© 2015 Macmillan Publishers Limited All rights reserved 0887-6924/15
www.nature.com/leu

ORIGINAL ARTICLE

Inhibition of plasmin attenuates murine acute graft-versus-host disease mortality by suppressing the matrix metalloproteinase-9-dependent inflammatory cytokine storm and effector cell trafficking

A Sato[1], C Nishida[1,2], K Sato-Kusubata[2], M Ishihara[1], Y Tashiro[1], I Gritli[1], H Shimazu[1], S Munakata[1], H Yagita[3], K Okumura[3], Y Tsuda[4], Y Okada[4], A Tojo[5], H Nakauchi[5], S Takahashi[5], B Heissig[2,3,6] and K Hattori[1,3,6]

The systemic inflammatory response observed during acute graft-versus-host disease (aGVHD) is driven by proinflammatory cytokines, a 'cytokine storm'. The function of plasmin in regulating the inflammatory response is not fully understood, and its role in the development of aGVHD remains unresolved. Here we show that plasmin is activated during the early phase of aGVHD in mice, and its activation correlated with aGVHD severity in humans. Pharmacological plasmin inhibition protected against aGVHD-associated lethality in mice. Mechanistically, plasmin inhibition impaired the infiltration of inflammatory cells, the release of membrane-associated proinflammatory cytokines including tumor necrosis factor-α (TNF-α) and Fas-ligand directly, or indirectly via matrix metalloproteinases (MMPs) and alters monocyte chemoattractant protein-1 (MCP-1) signaling. We propose that plasmin and potentially MMP-9 inhibition offers a novel therapeutic strategy to control the deadly cytokine storm in patients with aGVHD, thereby preventing tissue destruction.

Leukemia (2015) **29,** 145–156; doi:10.1038/leu.2014.151

INTRODUCTION

Allogeneic hematopoietic stem cell transplantation (allo-HSCT) is the only curative option for many hematological malignancies. However, the development of acute graft-versus-host disease (aGVHD) limits the success of allo-HSCT and is fatal in approximately 15% of transplant recipients. In the first phase of aGVHD, antigen-presenting cells are stimulated due to antigen disparities between host and graft.[1,2] Donor T cells are activated, and T-helper 1 (T_H1) cytokines like interferon-γ (IFN-γ), interleukin-2 (IL-2) and tumor necrosis factor-α (TNF-α) initiate the recruitment of effector cells (cytotoxic T lymphocytes, natural killer cells and monocytes). Finally, TNF-α, IL-1 and IFN-γ as inflammatory mediators induce end-organ damage. A network of soluble cytokines, a so-called 'cytokine storm', forms a critical link between each of these steps and may be responsible for the bulk of target-organ damage.[3] The 'cytokine storm' drives the systemic inflammatory response observed in septic shock and aGVHD, accelerates the coagulation/fibrinolytic system and generates an imbalance between coagulation and fibrinolysis.[4,5] Plasmin (plm), a serine protease, is generated by conversion from plasminogen (plg) by two plasminogen activators (PA), such as tissue-type PA (tPA) and urokinase-type PA (uPA). Although tPA has a dominant role in the resolution of fibrin clots (fibrinolysis), uPA can activate extracellular proteolysis during inflammatory processes.[6] Plm/plg binds to cells like monocytes via receptors (annexin 2 and Plg-R_{KT}),[7] can alter the expression of cytokines such as TNF-α, IL-1, IL-6 and monocyte chemoattractant protein-1 (MCP)-1[8–11] and modify cell migration.[12–14] The role of plm in guiding the cytokine storm is not well understood. Because plm can activate other proteases like metalloproteinases (MMPs)[15–17] and some MMP inhibitors can block processing of TNF-α and Fas-ligand (FasL),[18–22] we hypothesized that plm activation may control the cytokine storm and regulate the inflammatory response in murine models of aGVHD.

MATERIALS AND METHODS

Mice

Ten-week-old female C57BL/6 (B6; H-2^b) and six-week-old female (BALB/c × C57BL/6)F1 (CBF1; H-$2^{b/d}$) mice were purchased from Japan SLC Inc. (Hamamatsu, Japan). Ten-week-old female *Plg*$^{+/+}$ and *Plg*$^{-/-}$ mice, plasminogen activator inhibitor-1-deficient (*PAI1*$^{-/-}$) and *PAI1*$^{+/+}$ mice were used after more than 10 backcrosses onto C57BL/6 background. *Mmp9*$^{+/+}$ and *Mmp9*$^{-/-}$ mice were used after more than 10 backcrosses onto CD1 background. Animal protocols were approved by the Animal Review Board of The Institute of Medical Science, University of Tokyo.

Reagents

The plasmin inhibitor YO-2 [*trans*-4-aminomethylcyclohexanecarbonyl-Tyr(*O*-Pic)-octylamide] and YO-57 [*trans*-4-amiomethylcyclohexanecarbonyl-L-(*0*-picolyl)tyrosine-4-aminomethylanilide],[23,24] both provided by Yoshio Okada (Kobe Gakuin University, Kobe, Japan), were dissolved in

[1]Department of Stem Cell Regulation, Center for Stem Cell Biology and Regenerative Medicine, Institute of Medical Science at the University of Tokyo (IMSUT), Tokyo, Japan; [2]Department of Stem Cell Dynamics, Center for Stem Cell Biology and Regenerative Medicine, Institute of Medical Science at the University of Tokyo (IMSUT), Tokyo, Japan; [3]Department of Immunology, Atopy (Allergy) Research Center, Juntendo University School of Medicine, Tokyo, Japan; [4]Faculty of Pharmaceutical Sciences, Kobe Gakuin University, Kobe, Japan and [5]Department of Hematology and Oncology, Center for Stem Cell Biology and Regenerative Medicine, Tokyo, Japan. Correspondence: Dr K Hattori, Department of Stem Cell Regulation, Center for Stem Cell Biology and Regenerative Medicine, Institute of Medical Science at the University of Tokyo (IMSUT), 4-6-1, Shirokanedai, Minato-ku, Tokyo 108-8639, Japan.
E-mail: khattori@ims.u-tokyo.ac.jp
[6]These authors share senior authorship.
Received 21 November 2013; revised 1 April 2014; accepted 21 April 2014; accepted article preview online 5 May 2014; advance online publication, 3 June 2014

phosphate-buffered saline (PBS) at 375 μg/ml. The MMP inhibitor [N-hydroxy-2-((4-methoxysulfonyl)(3-pocolyl)-amino)-3- methylbutanamide (MMI270)] (Novartis Pharma Corporation, Basel, Switzerland)[25] was dissolved in dimethylsulfoxide at 10 mmol/l. The following reagents were used: D-(+)-galactosamine hydrochloride (GalN; Sigma-Aldrich, Tokyo, Japan), lipopolysaccharide (LPS; Sigma-Aldrich) from *Escherichia coli* 055:B5, mouse plg and plm (Innovative Research, Novi, MI, USA), recombinant human TNF-α (R&D Systems, Minneapolis, MN, USA).

Cell cultures

The human monocytic leukemia cell line THP-1 (3×10^5 cells/well) and the mouse monocytic leukemia cell line WEHI-274.1 (1×10^6 cells/well) were stimulated with 1 μg/ml LPS using 24-well Falcon plates (BD Biosciences, San Jose, CA, USA). A human FasL cDNA-transfected mouse T-lymphoma cell line (hFasL/L5178Y)[21,26] (1×10^6 cells/well) was cultured for 24 h.

Induction of lethal aGVHD

Bone marrow (BM) transplantation model: aGVHD was induced in lethally irradiated (8 Gy) CBF1 mice by intravenous injections of 1×10^7 BM cells and 5×10^7 splenocytes (SPs) from B6 mice on day 0. As a control, irradiated CBF1 mice were injected with the same number of BM cells and SPs from CBF1 mice. SP transfer model: CBF1 mice were intravenously injected with 2×10^8 SPs from B6 mice on day 0 and 7. Treatment: aGVHD mice were intraperitoneally injected with 3.75 mg/kg body weight (BW) of YO-2, YO-57 or PBS alone every day from days 0 to 28, day 0 to 14 or day 8 to 28.

Induction of lethal endotoxin shock

Mice were intraperitoneally injected with 400 mg/kg BW of GalN and 5 μg/kg BW of LPS (GalN/LPS). B6 mice were intraperitoneally injected with 3.75 mg/kg BW of YO-2 or PBS alone daily from day −5 to 2.

Enzyme-linked immunosorbent assay

Human TNF-α, FasL and plasmin inhibitor complex (PIC) were assayed in supernatants using commercial ELISA (enzyme-linked immunosorbent assay) kits (R&D Systems). Murine samples were assayed for TNF-α, IL-1β, FasL, MMP-9, IFN-γ, IL-6, MCP-1, plasmin-α2 antiplasmin complexes (PAP), uPA and tPA using ELISA kits (R&D Systems, BioLegend (San Diego, CA, USA), CUSABIO BIOTECH (Wuhan, China), Oxford Biomedical Research (Rochester Hills, MI, USA)).

aGVHD histopathology scoring

Tissues were fixed in 10% buffered formalin and embedded in paraffin. Hematoxylin and eosin stained tissue sections were evaluated using an OLYMPUS microscope and scored according to a published histopathological scoring system.[27] Standard magnifications were × 100/0.40 NA and × 200/0.75 NA.

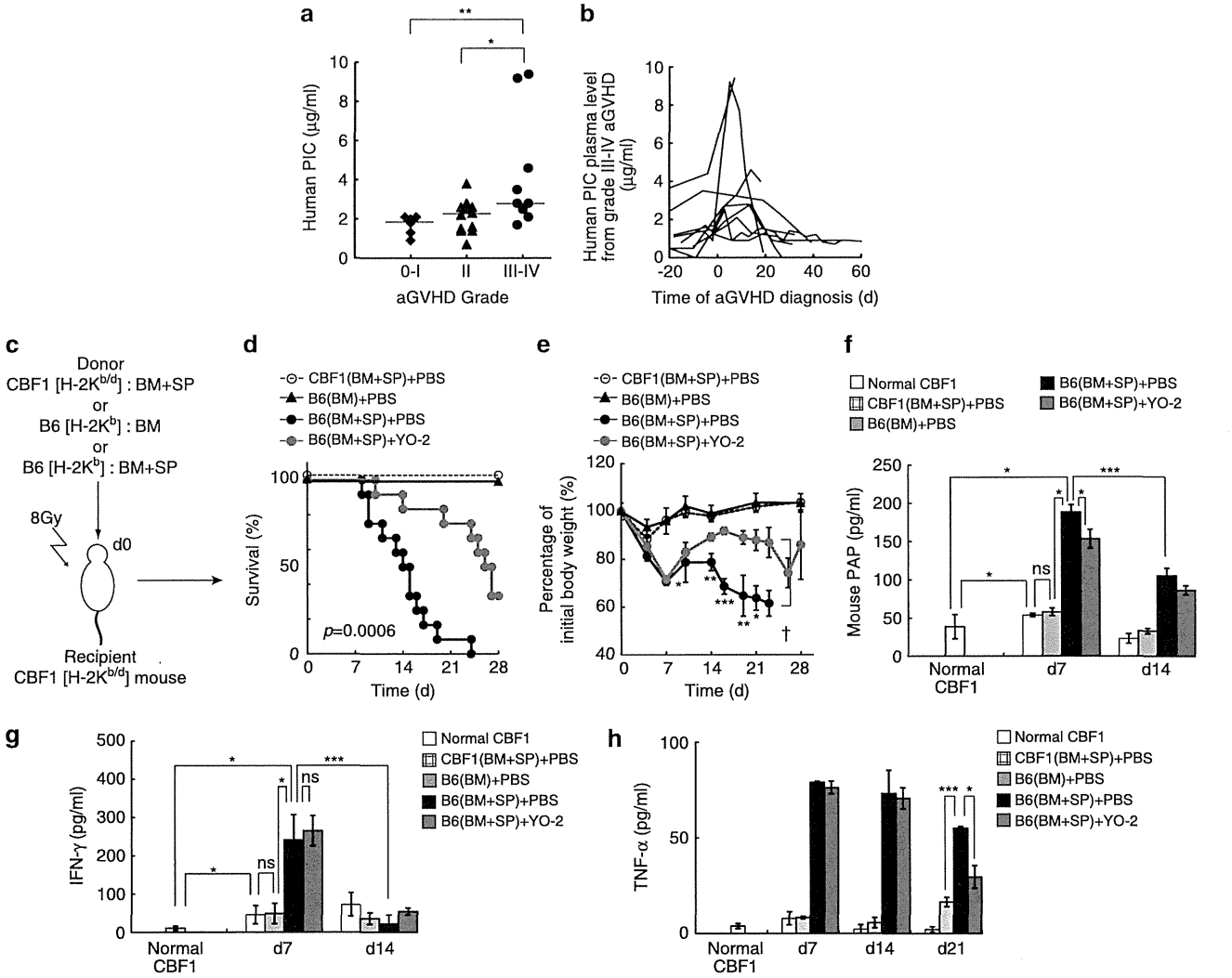

Figure 1. Plm is activated during the early phase of aGVHD. (**a**) ELISA of human PIC in plasma samples from human allo-HSCT recipients. (**b**) Human PIC plasma levels of patients with grade III–IV were plotted with day 0 set as the time of aGVHD onset. (**c–f**) aGVHD was induced in mice using a murine BM transplantation model. Mice were treated with PBS or YO-2 ($n = 12$/group). (**c**) Kaplan–Meier curves showing survival and (**e**) body weight. (**f**) ELISA of murine PAP ($n = 5$–11), (**g**) TNF-α ($n = 3$), and (**h**) IFN-γ ($n = 3$) in plasma at indicated times. Data represent mean ± s.e.m. from three independent experiments. $^*P < 0.05$, $^{**}P < 0.01$, $^{***}P < 0.001$.

© 2015 Macmillan Publishers Limited

Immunohistochemistry

Frozen murine tissue sections (5 μm) were washed with PBS, serum blocked and stained with the first antibody (Ab), overnight at 4 °C. Small intestine sections were stained with anti-CD11b Ab (1:50, clone M1/70; BD) followed by biotin-conjugated goat anti-rat IgG (1:200, CEDARLANW) and FITC-conjugated streptavidin (1:200, BD PharMingen, San Diego, CA, USA). Small intestine sections were stained with anti-CD3e Ab (1:50, BD PharMingen) followed by FITC-conjugate goat anti-armenian hamster IgG (H + L) (1:200, Abcam, Cambridge, MA, USA). Spleen sections were stained rabbit anti-murine MCP-1 (1:500, clone JE; PEPROTECH, Rocky Hill, NJ, USA)

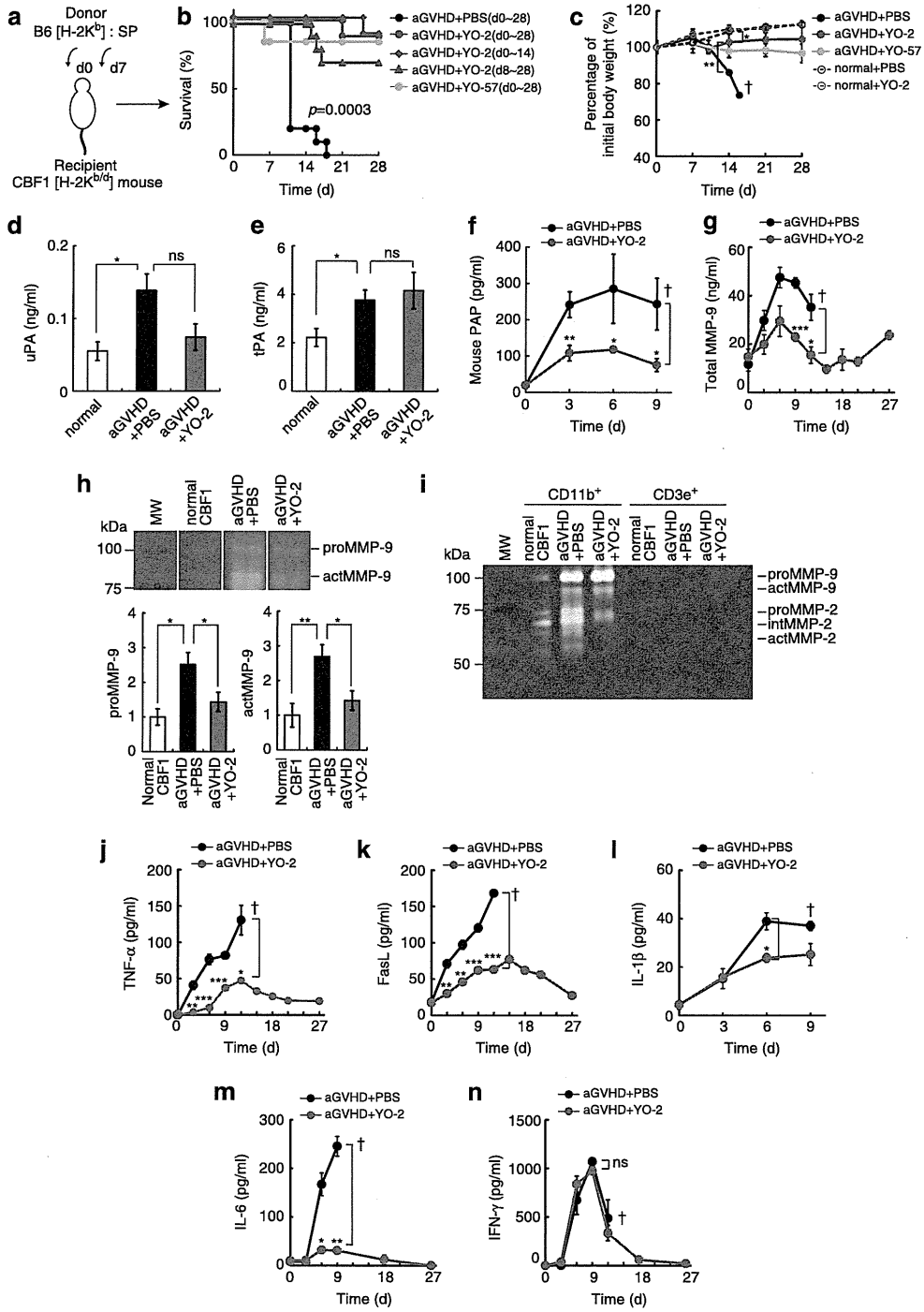

Figure 2. Plm inhibition protects against aGVHD-associated lethality by controlling proinflammatory cytokine/chemokine production. (**a**–**m**) aGVHD was induced in mice using a splenocytes (SPs) transfer model. Mice ($n = 10$/group) were treated with PBS, YO-2 and YO-57. Kaplan–Meier curves showing (**b**) survival and (**c**) body weight. ELISA of (**d**) uPA ($n = 3$) and (**e**) tPA ($n = 3$) in pooled plasma samples of three PBS- or YO-2-treated SP transfer model mice obtained at day 6. (**f**) Mouse PAP ($n = 7$–9) and (**g**) total MMP-9 ($n = 3$) were measured in plasma by ELISA. (**h**) Blood samples retrieved on day 6 were analyzed by gelatin zymography (upper panel). Quantification of the intensity of proMMP-9 and actMMP-9 bands (lower panel) ($n = 3$–4). (**i**) CD11b or CD3e positive FACS-sorted SPs from aGVHD mice at day 8 were cultured for 24 h. Culture supernatants were analyzed by gelatin zymography. (**j**) TNF-α, (**k**) FasL, (**l**) IL-1β, (**m**) IL-6 and (**n**) IFN-γ was measured by ELISA at indicated times in pooled plasma samples of PBS-and YO-2-treated aGVHD mice ($n = 3$/cytokines). Data represent mean ± s.e.m. from three independent experiments. $^*P < 0.05$, $^{**}P < 0.01$, $^{***}P < 0.001$. †Due to death no data available.

© 2015 Macmillan Publishers Limited

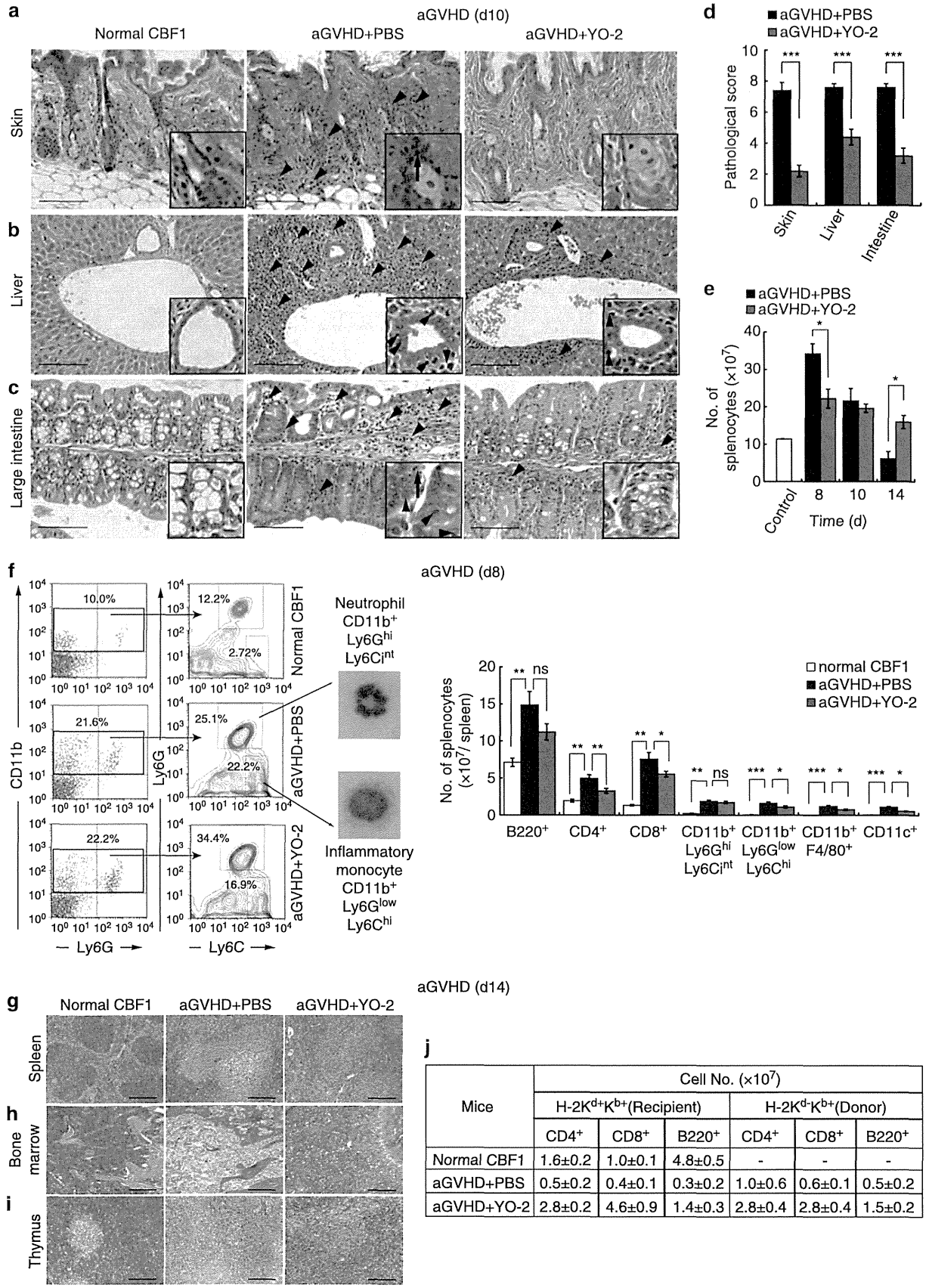

j

Mice	Cell No. (×10^7)					
	H-2K^d+K^b+(Recipient)			H-2K^d-K^b+(Donor)		
	CD4+	CD8+	B220+	CD4+	CD8+	B220+
Normal CBF1	1.6±0.2	1.0±0.1	4.8±0.5	-	-	-
aGVHD+PBS	0.5±0.2	0.4±0.1	0.3±0.2	1.0±0.6	0.6±0.1	0.5±0.2
aGVHD+YO-2	2.8±0.2	4.6±0.9	1.4±0.3	2.8±0.4	2.8±0.4	1.5±0.2

© 2015 Macmillan Publishers Limited

followed by Alexa Fluor 594 goat anti-rabbit IgG (H + L) (1:200, Invitrogen, Carlsbad, CA, USA), and costained with anti-CD31 Ab (1:500, clone ER-MP12; BMA Biomedicals, Augst, Switzerland) and biotin-conjugated goat anti-rat IgG (1:200, CEDARLNW) and Alexa Fluor 488 streptavidin (1:200, Invitrogen), or costained with anti-actin Ab (1:500, clone 3F10; GeneTex, Irvine, CA, USA) followed by Alexa Fluor 488 goat anti-mouse IgG (H + L) (1:200, Invitrogen).

WEHI-274.1 cells, after preincubation with 1 μg/ml of LPS with PBS or YO-2 for 2 h, were washed. Then cells were fixed with 4% PFA/PBS on slides and permeabilized with 0.1% Triton X-100/PBS after 30 min. Following blocking using 10% goat serum in PBS for 30 min, cells were incubated using anti-NFκB p65 (1:100; Santa Cruz, Dallas, TX, USA; sc-109) for 1 h in PBS with 1% BSA, washed three times with PBS, and incubated for 1 h with Alexa 594-conjugated goat anti-rabbit Ab (1:100; Invitrogen) in PBS with 1% BSA. After another washing step, cells were mounted with aqueous mounting medium.

Flow cytometric analysis

Cell-surface antigen analysis was performed by staining with the following Abs: goat anti-mouse CCR2 (AbD Serotec), CD4-PE, CD8a-PE, Gr-1-PE, Ly6G-PE, CD11c-PE, CD8a-FITC, F4/80-FITC, Ly6C-FITC, H2K^{d}-FITC B-220-APC, CD11b-APC, CD3e-APC, H-2K^{b}-biotin and APC streptavidin (BD PharMingen). Cells (1×10^{6}) were analyzed on a BD FACS Calibur.

PCR with reverse transcription analysis

Total RNA was extracted using Trizol (Invitrogen), and cDNA was generated according to the manufacturer's protocols. Specific forward and reverse primers, respectively, were designed as follows: human *TNF-α*: (5′-ttctccttcc tgatcgtg-3′) and (5′-agggctgattagagagaggt-3′); human *FasL*: (5′-gagagtctac cagccagatg-3′) and (5′-caggacaattccataggtgt-3′); human *uPA*: (5′-ccctcctctc ctccagaagaa -3′) and (5′-gtagacgatgtagtcctccttc-3′); human *uPAR*: (5′-ggtga cgccttcagcatga-3′) and (5′-cccactgcggtactggacat-3′); human *GAPDH* control: (5′-tggtctcctctgacttcaac-3′) and (5′-ctgttgctgtagccaaattc-3′); mouse *TNF-α*: (5′-gccgatttgctatctcatac-3′) and (5′-ggtatatgggctcataccag-3′); and mouse *β-actin* control: (5′-tggaatcctgtggcatccatgaaac-3′) and (5′-taaaacgca gctcagtaacagtccg-3′). Gene expression levels were measured using an ABI Prism 7500 sequence detection system (Applied Biosystems, Carlsbad, CA, USA).

Western blotting

Cells were lysed in lysis buffer (Cell Signaling Technology, Danvers, MA, USA). Recombinant murine MCP-1 (JE/CCL2, PEPROTECH) 50 nM were preincubated with 25 μM YO-2, followed by 7.15 IU/ml plm stimulation. Culture supernatants were removed after 30 min. Lysates/supernatants were separated by 16% Tricine-SDS–polyacrylamide gel electrophoresis and transferred to a PVDF membrane.[28] Membranes were immunoblotted with anti-TNF-α (1:1000; Cell Signaling Technology) and anti-β-tubulin (1:2000; Sigma-Aldrich) followed by HRP-conjugated or alkaline phosphatase-conjugated secondary Ab (1:500; Nichirei Bioscience, Tokyo, Japan). Membranes were immunoblotted with anti-mouse MCP-1 Ab (0.2 μg/ml; PEPROTECH) followed by HRP-conjugated secondary Ab (1:500; Nichirei Bioscience). Membranes were incubated with ECL-Plus (GE Healthcare Life Sciences, Piscataway, NJ, USA), and the chemiluminescent signal was detected on a LAS4000 (Fujifilm) according to the manufacturer's instructions. The alkaline phosphatase signal was detected using a Histofine Kit (Nichirei Bioscience).

Transwell migration assay

SPs derived from SP transfer mouse aGVHD model were isolated on 8 days after the initial transplantation, stained with CD11b-PE and CD3e-APC, and placed in the upper well of a 24-well transmigration chamber at 0.5×10^{6} cells per 0.1 ml (Corning, New York, NY, USA). Cells migrated for 2 h at 37 °C towards: 10 nM MCP-1 (JE/CCL2, PEPROTECH), ± 1.43 IU/ml plm and ± 5 μM YO-2. Migrated CD11b^{+} and CD3e^{+} subpopulations were calculated from the total number of SPs recovered and the percentages of CD11b^{+} and CD3e^{+} cells determined by FACS.

Zymography

MMP activity of plasma samples and culture supernatants was determined by gelatin zymography.[29,30] Density of each lytic band was quantified using image analysis software (ImageJ).

Chromogenic assay for plasmin activity

The kinetics of active plasmin formation was followed by measuring the release of *p*-nitroaniline from a chromogenic substrate (D-Val-Leu-Lys *p*-nitroanilide dihydrochloride, Sigma), detected as a change in absorbance (Δ405 nm/min) using a multiwell plate reader.

Plasma samples from the patients following HSCT

From January 2009 to June 2011, 27 patients underwent HSCT at the IMSUT. In accordance with the Declaration of Helsinki, patients gave their informed consent. We have obtained approval from the Ethics Committee of the IMSUT.

Statistical analysis

Survival curves were plotted using Kaplan–Meier estimates. We used the log-rank test for analysis of survival data and the Mann–Whitney *U*-test for statistical analysis of clinical scores. Student's *t*-test was used for statistical analysis of remaining data. Data are presented as means ± s.e.m. $P<0.05$ was considered statistically significant.

RESULTS

Plm is activated during the early phase of aGVHD

To investigate whether activation of plasmin (plm) occurs after HSCT and is associated with aGVHD, we analyzed patient plasma samples of human HSCT recipients. Patient demographics were compared (Supplementary Table 1) and the aGVHD severity was rated on a scale of Grade 0–I, Grade II and Grade III–IV (severe aGVHD). As a measure of plm activation, human plasmin α2-PIC plasma levels (around 0–100 days after transplantation) were determined. Individual maximum human PIC plasma levels correlated with the grade of aGVHD (Figure 1a). Human PIC levels peaked within the first 2 weeks after aGVHD diagnosis (Figure 1b) in circulation, which was followed by a decrease in plasminogen (plg), and an increase in thrombin–antithrombin and plasminogen activator inhibitor-1-tPA complex (PAI-1-tPA complex; Supplementary Figure 1). The clinical data indicated that plasmin activation was observed during early phase of severe aGVHD in humans.

Next, we studied the effect of plm inhibition during aGVHD progression in a murine major histocompatibility complex (MHC)-mismatched BM transplantation model of lethal aGVHD. CBF1 recipients received total body irradiation as a conditioning regimen followed by the transplantation of BM cells with or without SPs (Figure 1c). By day 21, SPs were of donor origin and blood counts had recovered (data not shown). Pharmacological plm inhibition was achieved using the plm inhibitor YO-2.[23,24] YO-2 inhibits plm by blocking the catalytic site, and efficiently inhibits circulating plm (Supplementary Figure 2a). YO-2 treatment delayed disease progression, showing improved survival and attenuated weight loss in mice (Figures 1d and e). Clinical signs of

Figure 3. Plm inhibition reduces aGVHD-associated tissue destruction, inflammatory changes and lymphoid hypoplasia. (**a–d**) Tissue sections from mice 8 days after SP transfer were stained with hematoxylin and eosin (H&E; scale bar, 100 μm). Representative images (× 200) of (**a**) skin, (**b**) liver and (**c**) large intestinal tissue sections show aGVHD-associated cell infiltration (arrow head), apoptotic body (arrow) and ulceration (asterisk). (**d**) Semi-quantitative histopathological scoring of tissues ($n = 5$/group). (**e**) Absolute numbers of SPs from mice following SP transfer determined at indicated times ($n = 5$). Data are the mean ± s.e.m. from three independent experiments. *$P<0.05$, **$P<0.01$ and ***$P<0.001$. (**f**) Absolute number of SP subpopulations calculated after obtaining the percentage of these cell populations by FACS. Spleens were harvested from CBF1, and PBS- or YO-2-treated aGVHD mice on day 8 ($n = 3$–5). (**g–i**) Tissue sections from mice 14 days after SP transfer were stained with H&E (scale bar, 200 μm). Representative images (× 100) of (**g**) spleen, (**h**) bone marrow and (**i**) thymus sections. (**j**) After determination of the percentages of each subpopulation by three-color FACS, the absolute cell numbers of CD4^{+} T, CD8^{+} T and B220^{+} B cells of host (H-2K^{d+}K^{b+}) or donor (H-2K^{d-}K^{b+}) origin in SPs from CBF1, PBS-treated or YO-2-treated aGVHD mice on day 14 were calculated from the total numbers of SPs recovered ($n = 3$). Data are representative from three independent experiments.

© 2015 Macmillan Publishers Limited

aGVHD did not occur in CBF1 recipients adoptively cotransferred with syngenic BM cells plus SP (CBF1:BM + SP) or allogenic C57Bl/6 (B6) BM cells (B6:BM), whereas aGVHD developed in CBF1 recipients transplanted with B6 BM cells and SP (B6:BM + SP). Even though all mice had received total body irradiation, plm activation as determined by the increase in circulating mouse PAP was low in

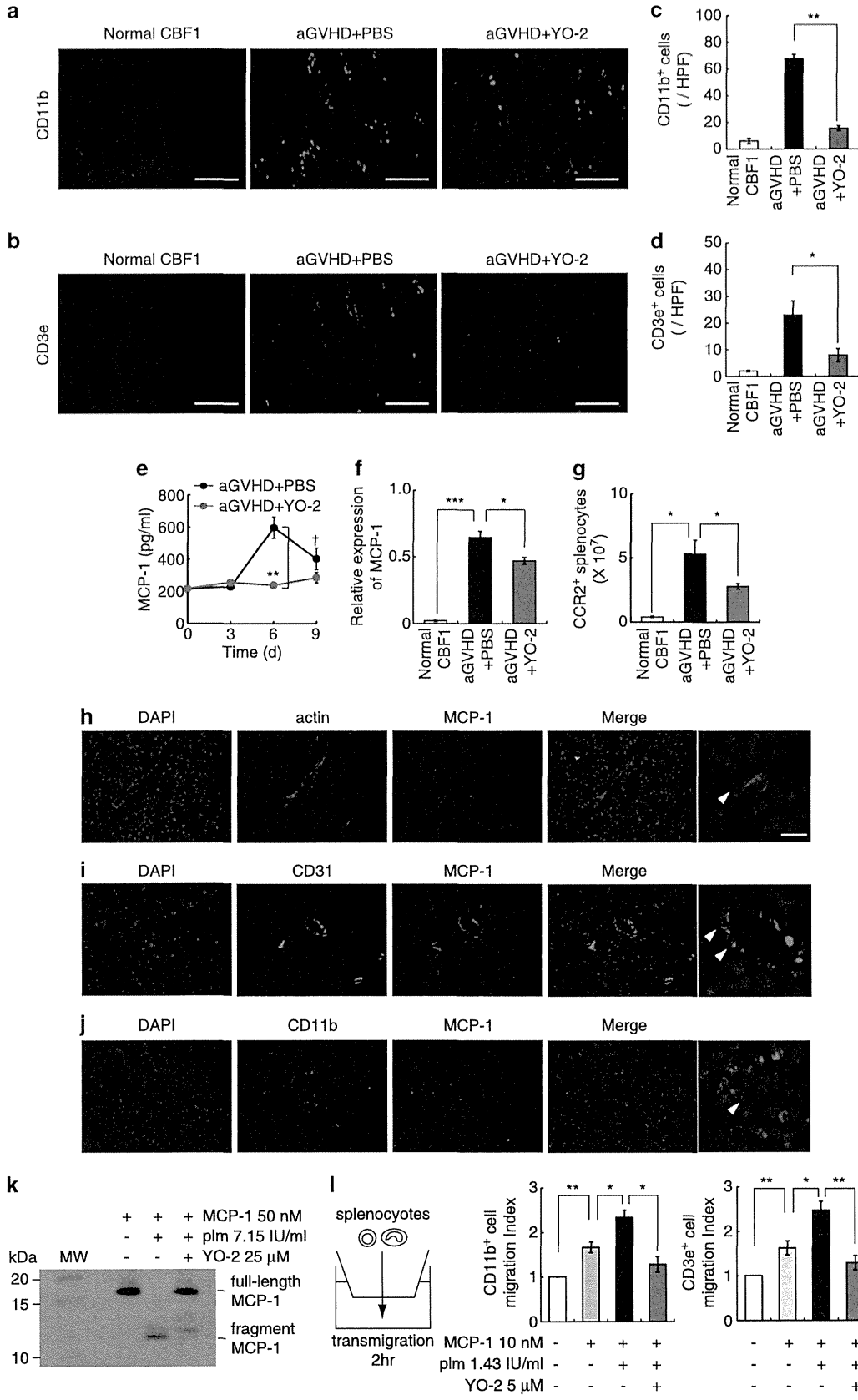

© 2015 Macmillan Publishers Limited

CBF1 recipients transplanted with CBF1:BM + SP or B6:BM cells (Figure 1f), indicating that total body irradiation alone was not sufficient to activate plm. In contrast, activation of plm was found in CBF1 mice receiving B6:BM + SP peaking on day 7 (Figure 1f).

T_H1 cytokines are released during aGVHD under MHC-mismatch conditions. T_H1 cytokines like TNF-α and IFN-γ were not upregulated in syngenic BM cells plus SP (CBF1:BM + SP) or allogenic C57Bl/6 (B6) BM cells (B6:BM) (Figures 1g and h). TNF-α production after aGVHD induction was suppressed in YO-2-treated aGVHD mice. These data suggest that plm occurred under MHC-mismatch conditions in the early phase of aGVHD and that plm and T_H1 cytokines peaked around day 7.

Plm inhibition protects against aGVHD-associated lethality by controlling proinflammatory cytokine/chemokine production

Because T-cell alloreactivity rather than irradiation seems to be important for plm activation, we next used another MHC-mismatched mouse model, a so-called 'parent-to-F1' model of lethal aGVHD (Figure 2a). Mixed chimerism was found in SPs of day 28 (data not shown). Because plm is activated mainly during the early phase of aGVHD, YO-2 was only injected from day 0 to 8 in this MHC-mismatched mouse aGVHD model. YO-2 treatment improved the survival and prevented aGVHD-associated BW loss in SPs transfer-induced aGVHD mice (Figures 2b and c). Even though YO-2 had been reported to induce thymocyte apoptosis *in vitro*, thymocytes isolated from YO-2-treated aGVHD animals did not show increased T-cell apoptosis (Supplementary Figure S2b). Next, we injected another plm inhibitor (YO-57), which had been reported to not affect thymocyte apoptosis. Similarly to YO-2 treatment, YO-57 treatment improved the survival and prevented aGVHD-associated BW loss (Figures 2b and c). These data indicate that plm inhibition rather than T-cell apoptosis seemed to be important to improve clinical symptoms of aGVHD *in vivo*. As signs of the activation of fibrinolysis during aGVHD progression, murine PAP, uPA and tPA plasma levels increased after transplantation (Figures 2d–f). PAP levels were low in YO-2-treated aGVHD mice. As the function of plm is to dissolve fibrin clots, and plm inhibition might cause fibrin deposition/clot formation, accelerate coagulation, d14 liver tissues from aGVHD mice were stained for fibrin(ogen). No difference in fibrin(ogen) staining pattern was observed in YO-2- and vehicle-treated aGVHD-derived tissues (Supplementary Figures S3a and b). Fibrin deposition was only found in tissues from $Plg^{-/-}$ mice. Similarly, no abnormal plasma levels of thrombin–antithrombin (Supplementary Figure S3c) were found after YO-2 treatment.

Increased serum levels of matrix metalloproteinase-9 (MMP-9) have been reported in aGVHD patients after allo-HSCT.[31] Plm inhibition partially prevented the rise in total plasma MMP-9 levels in circulation, with a decrease in both the pro-MMP and active form of MMP-9 as determined by zymography (Figures 2g and h). MMP-9 and MMP-2 proteolytic activity was high in $CD11b^+$, but not $CD3e^+$ FACS-sorted SPs of aGVHD mice (Figure 2i).

Because MMP-9 protein increased and active MMPs/MMP-9 can convert cytokines/chemokines into more active or inactive immune signals,[32] or can process membrane-bound proteins,[30,33] we hypothesized that plm inhibitor treatment can control cytokine processing. Circulating TNF-α, FasL, IL-1β and IL-6, but not IFN-γ levels were reduced in YO-2-treated aGVHD mice (Figures 2j–n). Plm addition increased gene transcription of *TNF-α*, *IL-1β*, *IL-6* and *MCP-1* in monocytes in a dose-dependent manner, a process that could be blocked when YO-2 was added to the cultures (Supplementary Figure S4a). These data indicate that blockade of the naturally occurring activation of plm during the early phase of aGVHD development impaired the production of cytokines/chemokines.

Plm inhibition reduces aGVHD-associated inflammatory changes

On day 10 after transplantation, skin from YO-2-treated aGVHD mice showed less cell infiltration, hyperkeratosis and loss of hair follicles, the liver showed less bile duct damage and portal cell infiltrates and the large intestines showed less cell infiltration, lamina propria inflammation, crypt destruction and mucosal atrophy when compared with PBS-treated aGVHD mice (Figures 3a–c). YO-2-treated mice compared with controls showed a lower disease score by histopathological evaluation (Figure 3d). We observed SP expansion 8 days after transplantation, followed by lymphoid hypoplasia 14 days after transplantation (Figure 3e). The numbers of T cells, $CD11b^+Ly6G^{low}Ly6C^{hi}$ inflammatory monocytes, $CD11b^+F4/80^+$ macrophages and $CD11c^+$ dendritic cells were decreased in YO-2-treated aGVHD mice compared with the PBS-treated aGVHD mice (Figure 3f). These findings demonstrate that pharmacological inhibition of plm delays aGVHD-associated skin, liver and intestine damage, and that it suppresses the infiltration of effector cells in aGVHD tissues.

Plm inhibition reduces lymphoid hypoplasia

GVHD-associated lymphoid hypoplasia and B-cell dysfunction has been shown to be dependent upon donor T cell-mediated function.[34] On day 14 after transplantation, when compared with PBS-treated aGVHD mice, the spleen from YO-2 treated aGVHD mice showed less lymphoid atrophy with decreased cellularity and structural disorganization, the BM showed less atrophy and a paucity of hematopoietic cells, and the thymus showed less disorganized demarcation between the thymic cortex and medulla (Figures 3g–i). In the SPs from YO-2-treated GVHD mice, $B220^+$ B cells of host or donor origin were preserved as compared with PBS-treated aGVHD mice (Figure 3j). These findings suggest that plm inhibition reduced lymphoid atrophy and immunosuppression associated with aGVHD.

Plasmin inhibition impairs MCP-1-mediated cell migration *in vitro*

During aGVHD reaction, donor T cells initially migrate to the spleen and peripheral lymphoid tissues within hours.[35] YO-2 treatment reduced the number of $CD11b^+$ cells and $CD3e^+$ T effector cells as determined by immunohistochemistry on spleen sections after 8 days of aGVHD initiation (Figures 4a–d). Because T cell and inflammatory cell trafficking into parenchymal organs requires specific selectin–ligand, integrin–ligand[36] and chemokine–receptor interactions, for example, MCP-1 with its receptor CCR2, we next examined whether plm could alter MCP-1/CCR2 signaling. YO-2-treated aGVHD mice showed lower

Figure 4. Plm inhibition influences both the initial T-cell expansion and its concomitant effector cell migration to aGVHD target organs. (**a–d**) Immunofluorescent staining of (**a**) CD11b and (**b**) CD3e of intestinal tissue derived from CBF1 mice and PBS of YO-2-treated aGVHD mice 8 days after SP transfer (scale bar, 100 μm). Quantification of (**c**) $CD11b^+$ and (**d**) $CD3e^+$ cells in intestinal tissues ($n = 3$/group). (**e**) ELISA of MCP-1 in pooled plasma samples of three SP transfer model mice obtained at indicated times. (**f**) *MCP-1* gene expression in spleen on day 8 was determined by qPCR ($n = 3$) (**g**) $CCR2^+$ cells within SPs harvested from mice after SP transfer on day 8 ($n = 3$–4) were determined by FACS. (**h–j**) MCP-1 was costained with (**h**) actin, (**i**) CD31 and (**j**) CD11b on spleen sections derived from PBS-treated aGVHD mice 8 days after SP transfer (scale bar, 10 μm; $n = 3$). (**k**) Western blot analysis of MCP-1 after incubation of recombinant (rec.) murine MCP-1with/without plasmin in the presence/absence of YO-2 ($n = 3$). (**l**) Transmigration assay of $CD11b^+$ or $CD3e^+$ SPs migrating towards medium in the lower chamber containing MCP-1 in the presence or absence of rec. plasmin with or without YO-2 (right; $n = 3$). Each experimental condition was assayed in triplicate. Data represent mean ± s.e.m from three independent experiments. *P*-values: PBS versus YO-2: $^*P < 0.05$, $^{**}P < 0.01$, $^{***}P < 0.001$.

© 2015 Macmillan Publishers Limited

MCP-1 plasma levels (Figure 4e), MCP-1 mRNA expression in the spleen (Figure 4f) and a lower number of $CCR2^+$ cells in SPs when compared with PBS controls (Figure 4g). MCP-1 has been shown to be important for monocyte/macrophage, memory T cells and dendritic cells recruitment in several inflammatory models.[37,38] Immunohistochemical analysis identified $actin^+$, most likely smooth muscle cells/pericytes and $CD31^+$ endothelial cells as the major cellular source for MCP-1 in spleen sections of aGVHD mice (Figures 4h–j). Plm can enhance MCP-1 signaling by releasing a MCP-1 fragment with improved chemoattractive ability.[39,40] YO-2 prevented the release of the MCP-1 fragment as determined by western blot analysis, and blocked the improved chemoattractive ability of plm-processed MCP-1 using $CD11b^+$ or $CD3e^+$ cells, derived from the spleens of aGVHD mice *in vitro* (Figures 4k and l).

Plm inhibition protects against lethal endotoxin shock and reduced MMP-9 and TNF-α production *in vivo*

We next examined whether plm inhibition can control TNF-α production through MMPs. Administration of GalN/LPS is a model of endotoxin shock that is governed by monocyte/macrophage-released TNF-α. YO-2-treated B6 mice and $Plg^{-/-}$

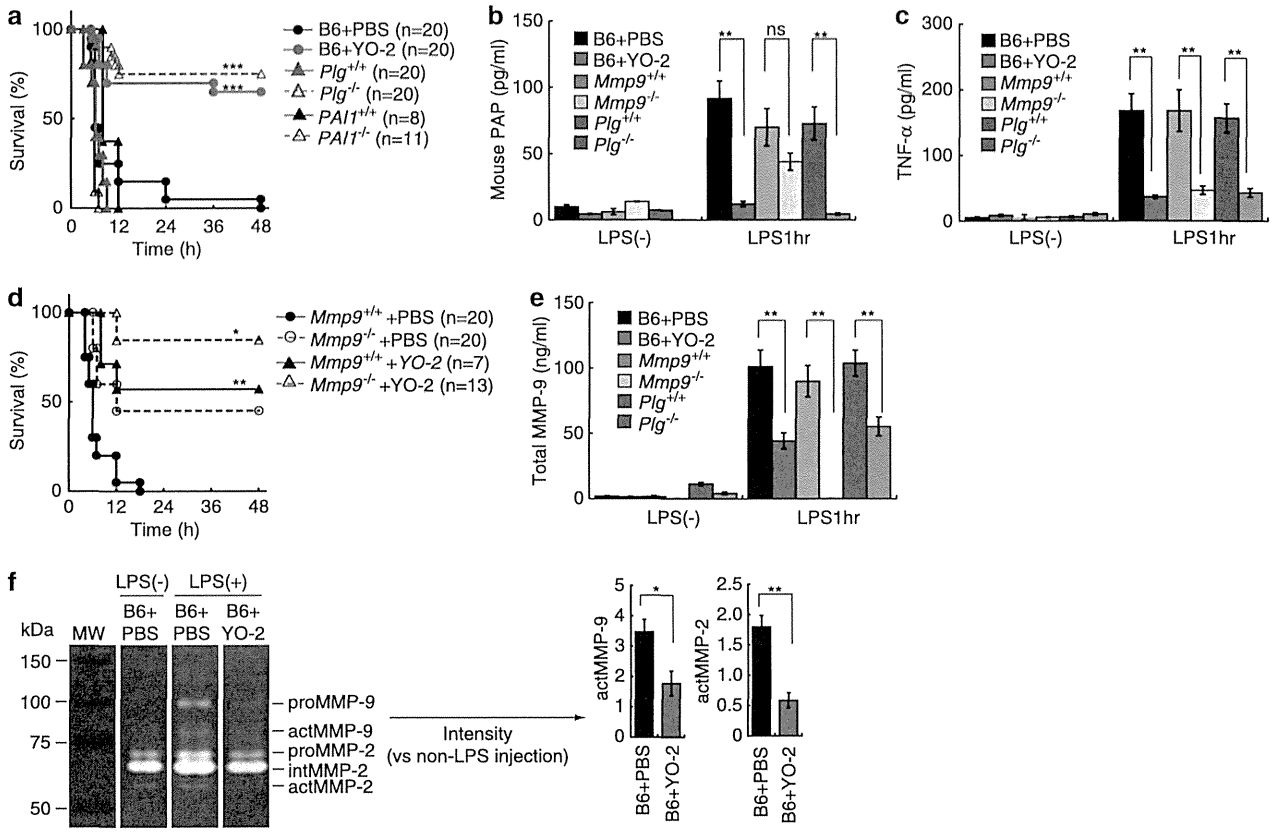

Figure 5. Plm inhibition protects against lethal endotoxin shock. (**a**) Kaplan–Meier curves showing survival of WT B6 mice treated with PBS or YO-2, $Plg^{+/+}$, $Plg^{-/-}$, $PAI1^{-/-}$ and $PAI1^{-/-}$ mice ($n=8$–20/group). Significant differences were found between B6 mice treated with PBS and YO-2: $^{***}P<0.001$; between $Plg^{+/+}$ and $Plg^{-/-}$ mice: $^{***}P<0.001$. (**b**, **c**) Sera and plasma were collected at 1 h after GalN/LPS injection. (**b**) PAP ($n=6$–10) and (**c**) TNF-α ($n=6$–15) were analyzed in plasma derived from GalN/LPS-injected mice by ELISA. (**d**) Kaplan–Meier curve showing survival of $Mmp9^{+/+}$, $Mmp9^{-/-}$ mice treated with or without YO-2 ($n=13$–20/group). Significant differences were found between $Mmp9^{+/+}$ and $Mmp9^{-/-}$ mice with PBS: $^{**}P<0.01$; between $Mmp9^{-/-}$ treated with PBS and YO-2: $^{*}P<0.05$. (**e**, **f**) Plasma samples were collected at 1 h after GalN/LPS injection. (**e**) Total MMP-9 ($n=5$) in plasma was measured by ELISA. (**f**) Blood samples were analyzed by gelatin zymography (left). Quantification of the intensity of actMMP-9 and actMMP-2 bands (right; $n=3$). Data represent the mean ± s.e.m. from two independent experiments. $^{*}P<0.05$, $^{**}P<0.01$, $^{***}P<0.001$.

Figure 6. Plm inhibition prevents TNF-α shedding and FasL production. (**a**, **b**) THP-1 monocytes were stimulated by 5 ng rhTNF-α, 1 μg/ml LPS and 20 ng rIFN-γ for 2 h. (**a**) *uPA* and (**b**) *uPAR* gene expressions in cultured cells were determined by qPCR ($n=3$). (**b**, **c**) Dose-responsive inhibition of cytokine release from LPS-stimulated THP-1 and hFasL/L5178Y cells by YO-2. TNF-α and FasL levels were determined in culture supernatants by ELISA ($n=3$). (**d**) Gene expression of cytokines in cultured cells as determined by qPCR ($n=3$). (**e**–**i**) WEHI-274.1 cells were preincubated with 0.5 μM mouse plasminogen and 5 μM YO-2, 5 μM MMI270 or PBS, followed by 1 μg/ml LPS stimulation in the absence of serum. (**e**) Plm in culture supernatants was detected using a plm chromogenic substrate ($n=3$). (**f**) Quantitation of relative intensity of proMMP-9 and actMMP-9 bands in supernatants as determined by zymography ($n=3$). (**g**) Secreted TNF-α were determined by ELISA ($n=3$). (**h**) *TNF-α* gene expression in cultured cells as determined by qPCR ($n=3$). (**i**) Confocal immunofluorescence staining of NF-κB (p65) in LPS-stimulated WEHI-274.1 cells (scale bar, 10 μm). (**j**) Left: western blot of membrane-TNF-α (mTNF-α) in cell lysates ($n=3$). Right: quantification of mTNF-α relative to β-tubulin. (**k**) Proposed mechanism by which plm exacerbates the cytokine storm in inflammatory diseases. Inflammatory cells like monocytes, by releasing the plasminogen activator uPA catalyze the generation of plm. Plm by activating other MMPs can generate a proteolytic environment resulting in the shedding of TNF-α and in an increased production of other cytokines, thereby fueling the so-called 'cytokine storm'. As cytokines in turn can promote the production of inflammatory cells, a vicious cycle is initiated. In addition, plm promotes the recruitment of inflammatory cells, such as $CCR2^+$ by generating a MCP-1 fragment with improved chemoattractive properties. Data represent the mean ± s.e.m. from three independent experiments. $^{*}P<0.05$, $^{**}P<0.01$, $^{***}P<0.001$.

© 2015 Macmillan Publishers Limited

mice, but not *PAI1*$^{-/-}$ mice, were protected against lethal endotoxin shock (Figure 5a). We found high PAP plasma levels in PBS-treated B6 mice 2 h after LPS injection, indicating that plm is activated in the early phase after LPS injection. PAP plasma levels were decreased in YO-2-treated B6 mice and *Plg*$^{-/-}$ mice, but not *Mmp9*$^{-/-}$ mice (Figure 5b). A reduction in circulating PAP levels was observed, but this did not reach significance in *Mmp9*$^{-/-}$ mice. We determined whether TNF-α levels were reduced after GalN/LPS injection. Indeed, YO-2-treated B6 mice and *Plg*$^{-/-}$ and *Mmp9*$^{-/-}$ mice showed decreased TNF-α plasma levels (Figure 5c). YO-2 treatment could not prevent death in mice that were intravenously injected with recombinant mouse TNF-α (data not shown). These results indicate that plm is activated during the early phase after the onset of endotoxin shock and that plm inhibition blocks the release of TNF-α *in vivo*.

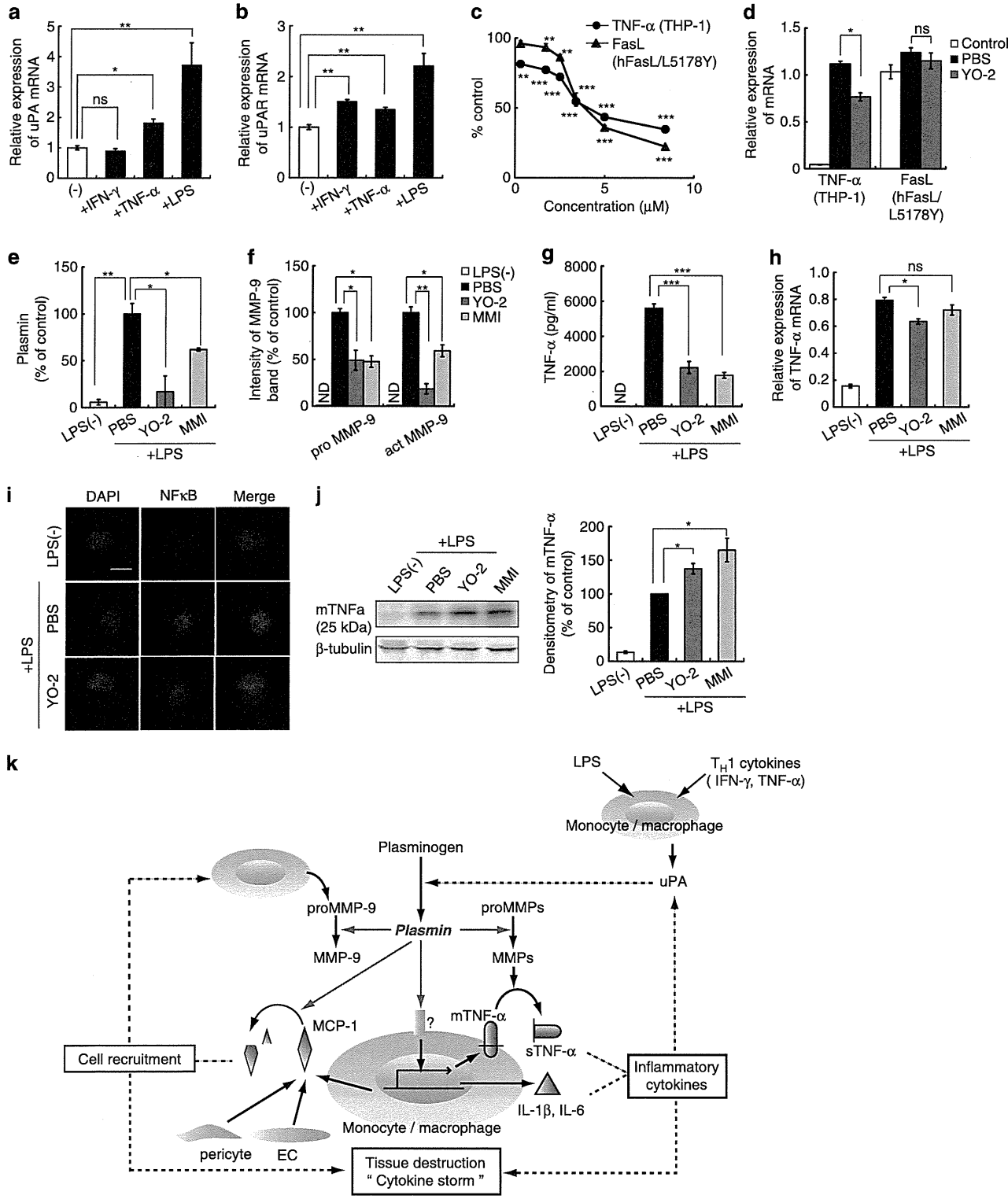

© 2015 Macmillan Publishers Limited

Next, we tested whether plm-mediated lethality and TNF-α production required endogenous MMP-9 in a model of endotoxin shock. *Mmp9*$^{-/-}$ mice were partially resistant to endotoxin shock-associated lethality (Figure 5d). These data suggest that plm inhibition prevents TNF-α production in part through MMP-9.

YO-2 treatment restored survival in GalN/LPS-injected *Mmp9*$^{-/-}$ mice (Figure 5d). YO-2 treatment reduced the total amount of MMP-9 and active MMP-9 and MMP-2 protein in circulation, as determined by ELISA and zymography (Figures 5e and f). As plm inhibition inactivates not only MMP-9, but also other MMPs (like for example, MMP-2 as shown here), the survival-enhancing effects of plm inhibition after LPS administration is both MMP-9-dependent and MMP-9-independent.

Plm inhibition prevents TNF-α shedding and FasL production *in vitro*

We next examined the influence of T_H1 cytokines on the expression of fibrinolytic factors in monocytes/macrophages *in vitro*. The addition of LPS and TNF-α increased the expression of uPA (Figure 6a), whereas LPS, TNF-α and IFN-γ augmented uPAR expression in THP-1 cells (Figure 6b). These data indicate that inflammatory T_H1 cytokines enhance the gene expression of fibrinolytic factors in monocytes/macrophages. YO-2 inhibited the release of TNF-α and FasL in monocyte culture supernatants in a dose-dependent manner (Figure 6c). The reduction of FasL release was not the result of impaired gene expression, as shown by qPCR (Figure 6d), but rather seems to be due to impaired protein release of the cytokine.

When WEHI-274.1 cells were maintained in serum-free medium, plm and MMP-9 activity increased in culture supernatant after LPS stimulation, but was inhibited in cultures treated with YO-2 or the MMP inhibitor MMI270 (Figures 6e and f). TNF-α secretion from WEHI-274.1 cells was blocked by either YO-2 or MMI270 (Figure 6g). *TNF-α* mRNA accumulation in LPS-stimulated WEHI-274.1 cells was reduced by YO-2, but was not affected by MMI270 (Figure 6h). Plm-mediated upregulation of cytokines in human monocytes has been reported to involve NF-κB activation.[8] After LPS stimulation, p65 subunit of the transcription factor NF-κB immunofluorescence staining was localized in the nucleus in control cultures, but was detected in the cytosolic compartment in YO-2-treated cells (Figure 6i). These data suggest that YO-2 blocked plm-mediated NF-κB translocation to the nucleus, thereby blocking gene expression. Next we investigated whether plm induces TNF-α shedding from its 25-kDa membrane-associated form (mTNF-α) to its 17-kDa secretory form. Both YO-2 and MMI270 treatment enhanced the expression of 25-kDa mTNF-α as determined by western blot analysis (Figure 6j). These data indicate that plm accelerates the ectodomain shedding of mTNF-α *in vitro*, and can regulate its transcription.

We show that pharmacological plm inhibition prevents inflammation-associated lethality and tissue destruction in models of endotoxin shock and aGVHD (Figure 6k) by impairing the release of inflammatory cytokines/chemokines, which will further attract inflammatory cells or fuel the influx of inflammatory cells.

DISCUSSION

Here, we show that plm is activated during the early phase of endotoxin shock and aGVHD in mice and humans. Plm inhibition protects against the proinflammatory cytokine storm in these inflammatory diseases by blocking cytokine/chemokine production and inflammatory cell infiltration.

Donor T cells recognize MHC and their associated peptides on host APCs, which results in T-cell activation and T_H1 cytokine production. T_H1 cytokines increase due to a reaction between MHC-mismatch donor T cells and recipient APC, or LPS-activated APC including monocyte/macrophage. We observed that plm peak levels coincided with a peak in IFN-γ levels, a cytokine, mainly released by activated T cells. We therefore suspected that there is a link between T_H1 cytokines and plm activation. Monocytes exposed to IFN-γ and TNF-α upregulated the expression of the fibrinolytic factors uPA and uPAR. uPA binding to its receptor uPAR will convert more plg into plm. The newly produced plm will further increase the production of proinflammatory cytokines, establishing a vicious cycle of plm activation and cytokine production.

We provide evidence that plm inhibition blocks shedding of the membrane-associated proapoptotic cytokine TNF-α after LPS stimulation *in vitro* and promotes the release of FasL. Plm has been reported to cleave FasL, releasing a soluble proapoptotic FasL fragment from the surface of endothelial cells. The Fas/FasL pathway is particularly important in hepatic GVHD. Plm inhibitor treatment improved the pathological score in liver tissues of aGVHD mice. Similar to reports by others,[8,9] we show that plm inhibition inhibited the transcription of TNF-α,IL-1β, IL-6 and MCP-1 in monocytes by activating the NF-κB pathway. These data indicate that plm inhibition controls cytokine/chemokine production by blocking the processing and transcription.

Plm inhibition decreased the total amount of circulating MMP-9 in murine models of septic shock and aGVHD, and in a partial MMP-9-dependent manner improved survival in a murine septic shock model. Plasmin, via activation of MMP-3 is a potent activator of pro-MMP-9 *in vitro*.[41] In an experimental model of the autoimmune disease bullous pemphigoid, it was reported that plm, in concert with other unidentified mechanism(s) caused MMP-9 activation.[42] How can we explain the impaired rise in circulating MMP-9 after plm inhibition? One possibility is that plm as shown by others and us induces IL-1β, TNF-α production in monocytes.[8] These cytokines, like reported for IL-1β,[43] in turn can induce MMP-9. Plm inhibition prevented the cytokine increase.

Another scenario is that plm regulates the infiltration of MMP-9 producing cells in inflamed tissues during aGVHD. We identified $CD11b^+$ cells as major supplier of MMP-9 during aGVHD. The increase in total numbers of $CD11b^+$ cells, rather than changes on a cellular basis, most likely accounts for the net MMP-9 activation.

We show that plm improves MCP-1-mediated $CD11b^+$ and $CD3e^+$ cell migration *in vitro*. We found that MCP-1 gene transcription and protein release are reduced in YO-2-treated aGVHD mice *in vivo*. Furthermore, we confirmed and extended a report demonstrating that plm proteolytically removes the C terminus of MCP-1 thereby enhancing the chemotactic potency of MCP-1.[39,40] Even though we focused on MCP-1, other chemotactic molecules or alterations in the proteolytic environment by plm might contribute to the observed impaired myeloid cell recruitment into inflamed tissues. Coagulation is highlighted during septic shock and aGVHD. The serine proteinase activated protein C reduces mortality in animal models of sepsis,[44] and inhibits coagulation by blocking PAI-1 activity.[45,46] Often inflammatory diseases are associated with an increase in PAI-1 plasma levels, indicating that fibrinolysis is blocked during disease progression. On the other hand, increased tPA levels have been reported during sepsis in mice and the early phase of HSCT in humans.[5,47–49] We found that plm is activated during the early phase of aGVHD and endotoxin shock, causing severe tissue destruction. YO-2 can block excessive circulating plm thereby blocking fibrinolysis, without the requirement of binding to the lysine-binding site of the plg molecule-binding fibrin as other plm inhibitors. Clinically, patients often show signs of excessive fibrinolysis and coagulation at the same time. Especially in these cases, YO-2 treatment seems to be a good choice in cases with known risk of bleeding while using fibrinolysis-activating agents.

During sepsis, patients die from bacteremia or sepsis-induced hyperinflammation due to an uncontrolled 'cytokine storm'. During the late phase of immunosuppression, patients often die due to secondary infection.[50,51] These observations gave the rationale to conduct clinical studies to block proinflammatory

© 2015 Macmillan Publishers Limited

cytokines during sepsis and aGVHD. But the results have been disappointing due to immunosuppressive side effects.[51,52] We propose that pharmacological plm inhibition in the early profibrinolytic phase regulates the fatal cytokine storm without immunosuppressive side effects. Blockade of the activation of plm during the early phase of aGVHD development delays the onset of aGVHD, but is followed by a phase of the activation of the coagulation system demonstrating that there is an important therapeutic window to benefit from plm inhibition in the treatment of aGVHD.

The matrix-degrading PA/plm system is a general proteolytic enzyme system which mediates tissue destruction in, for example, sepsis,[53] group A streptococcus infection,[54] influenza virus infection[55] and in autoimmune inflammatory diseases. We propose that plm is a novel therapeutic target and biomarker for these diseases, where tissue destruction impairs the life quality of patients.

CONFLICT OF INTEREST

The authors declare no conflict of interest.

ACKNOWLEDGEMENTS

We thank physicians and nurses who cared for the patients and the staff of the FACS core facility at the IMST for their help, and Douaa Dhari for proof-reading of the manuscript. This work was supported by grants from a Grants-in-Aid for Scientific Research (C) from JSPS (KH; BH), a Grant-in-Aid for Scientific Research on Priority Areas from MEXT (KH), a Grant-in-Aid for Scientific Research from MHLW (KH; ST), Mitsubishi Pharma Research Foundation (KH), SENSHIN Medical Research Foundation (KH), Kyowa Hakko Kirin Co., Ltd. (KH), The NOVARATIS Foundation (Japan) for the Promotion of Science (BH) and a Grant-in-Aid for Scientific Research on Innovative Areas from MEXT (BH), Japan.

REFERENCES

1 Cooke KR, Hill GR, Crawford JM, Bungard D, Brinson YS, Delmonte J Jr *et al.* Tumor necrosis factor- alpha production to lipopolysaccharide stimulation by donor cells predicts the severity of experimental acute graft-versus-host disease. *J Clin Invest* 1998; **102**: 1882–1891.
2 Hill GR, Ferrara JL. The primacy of the gastrointestinal tract as a target organ of acute graft-versus-host disease: rationale for the use of cytokine shields in allogeneic bone marrow transplantation. *Blood* 2000; **95**: 2754–2759.
3 Teshima T, Ordemann R, Reddy P, Gagin S, Liu C, Cooke KR *et al.* Acute graft-versus-host disease does not require alloantigen expression on host epithelium. *Nat Med* 2002; **8**: 575–581.
4 Yiu HH, Graham AL, Stengel RF. Dynamics of a cytokine storm. *PLoS One* 2012; **7**: e45027.
5 Pinomaki A, Volin L, Joutsi-Korhonen L, Virtanen JO, Lemponen M, Ruutu T *et al.* Early thrombin generation and impaired fibrinolysis after SCT associate with acute GVHD. *Bone Marrow Transplant* 2010; **45**: 730–737.
6 Syrovets T, Simmet T. Novel aspects and new roles for the serine protease plasmin. *Cell Mol Life Sci* 2004; **61**: 873–885.
7 Lighvani S, Baik N, Diggs JE, Khaldoyanidi S, Parmer RJ, Miles LA. Regulation of macrophage migration by a novel plasminogen receptor Plg-R KT. *Blood* 2011; **118**: 5622–5630.
8 Syrovets T, Jendrach M, Rohwedder A, Schüle A, Simmet T. Plasmin-induced expression of cytokines and tissue factor in human monocytes involves AP-1 and IKKβ-mediated NF-κB activation. *Blood* 2001; **97**: 3941–3950.
9 Ward JR, Dower SK, Whyte MK, Buttle DJ, Sabroe I. Potentiation of TLR4 signalling by plasmin activity. *Biochem Biophys Res Commun* 2006; **341**: 299–303.
10 Li Q, Laumonnier Y, Syrovets T, Simmet T. Plasmin triggers cytokine induction in human monocyte-derived macrophages. *Arterioscler Thromb Vasc Biol* 2007; **27**: 1383–1389.
11 Burysek L, Syrovets T, Simmet T. The serine protease plasmin triggers expression of MCP-1 and CD40 in human primary monocytes via activation of p38 MAPK and janus kinase (JAK)/STAT signaling pathways. *J Biol Chem* 2002; **277**: 33509–33517.
12 Ohki M, Ohki Y, Ishihara M, Nishida C, Tashiro Y, Akiyama H *et al.* Tissue type plasminogen activator regulates myeloid-cell dependent neoangiogenesis during tissue regeneration. *Blood* 2010; **115**: 4302–4312.
13 Tashiro Y, Nishida C, Sato-Kusubata K, Ohki-Koizumi M, Ishihara M, Sato A *et al.* Inhibition of PAI-1 induces neutrophil-driven neoangiogenesis and promotes tissue regeneration via production of angiocrine factors in mice. *Blood* 2012; **119**: 6382–6393.
14 Gong Y, Hart E, Shchurin A, Hoover-Plow J. Inflammatory macrophage migration requires MMP-9 activation by plasminogen in mice. *J Clin Invest* 2008; **118**: 3012–3024.
15 Ishihara M, Nishida C, Tashiro Y, Gritli I, Rosenkvist J, Koizumi M *et al.* Plasmin inhibitor reduces T-cell lymphoid tumor growth by suppressing matrix metalloproteinase-9-dependent CD11b(+)/F4/80(+) myeloid cell recruitment. *Leukemia* 2012; **26**: 332–339.
16 Heissig B, Lund LR, Akiyama H, Ohki M, Morita Y, Romer J *et al.* The plasminogen fibrinolytic pathway is required for hematopoietic regeneration. *Cell Stem Cell* 2007; **1**: 658–670.
17 Heissig B, Ohki-Koizumi M, Tashiro Y, Gritli I, Sato-Kusubata K, Hattori K. New functions of the fibrinolytic system in bone marrow cell-derived angiogenesis. *Int J Hematol* 2012; **95**: 131–137.
18 Gearing AJ, Beckett P, Christodoulou M, Churchill M, Clements J, Davidson AH *et al.* Processing of tumour necrosis factor-alpha precursor by metalloproteinases. *Nature* 1994; **370**: 555–557.
19 McGeehan GM, Becherer JD, Bast Jr. RC, Boyer CM, Champion B, Connolly KM *et al.* Regulation of tumour necrosis factor-alpha processing by a metalloproteinase inhibitor. *Nature* 1994; **370**: 558–561.
20 Bajou K, Peng H, Laug W, Maillard C, Noel A, Foidart J *et al.* Plasminogen activator inhibitor-1 protects endothelial cells from FasL-mediated apoptosis. *Cancer Cell* 2008; **14**: 324–334.
21 Hattori K, Hirano T, Ushiyama C, Miyajima H, Yamakawa N, Ebata T *et al.* A metalloproteinase inhibitor prevents lethal acute graft-versus-host disease in mice. *Blood* 1997; **90**: 542–548.
22 Hattori K, Hirano T, Ushiyama C, Miyajima H, Yamakawa N, Ikeda S *et al.* A metalloproteinase inhibitor prevents acute graft-versus-host disease in mice after bone marrow transplantation. *Bone Marrow Transplant* 1999; **23**: 1283–1289.
23 Enomoto R, Sugahara C, Komai T, Suzuki C, Kinoshita N, Hosoda A *et al.* The structure-activity relationship of various YO compounds, novel plasmin inhibitors, in the apoptosis induction. *Biochim Biophys Acta* 2004; **1674**: 291–298.
24 Tsuda Y, Tada M, Wanaka K, Okamoto U, Hijikata-Okunomiya A, Okamoto S *et al.* Structure-inhibitory activity relationship of plasmin and plasma kallikrein inhibitors. *Chem Pharm Bull (Tokyo)* 2001; **49**: 1457–1463.
25 Peterson JT. Matrix metalloproteinase inhibitor development and the remodeling of drug discovery. *Heart Fail Rev* 2004; **9**: 63–79.
26 Kayagaki N, Kawasaki A, Ebata T, Ohmoto H, Ikeda S, Inoue S *et al.* Metalloproteinase-mediated release of human Fas ligand. *J Exp Med* 1995; **182**: 1777–1783.
27 Kaplan DH, Anderson BE, McNiff JM, Jain D, Shlomchik MJ, Shlomchik WD. Target antigens determine graft-versus-host disease phenotype. *J Immunol* 2004; **173**: 5467–5475.
28 Schagger H. Tricine-SDS-PAGE. *Nat Protoc* 2006; **1**: 16–22.
29 Lane WJ, Dias S, Hattori K, Heissig B, Choy M, Rabbany SY *et al.* Stromal-derived factor 1-induced megakaryocyte migration and platelet production is dependent on matrix metalloproteinases. *Blood* 2000; **96**: 4152–4159.
30 Heissig B, Hattori K, Dias S, Friedrich M, Ferris B, Hackett NR *et al.* Recruitment of stem and progenitor cells from the bone marrow niche requires MMP-9 mediated release of kit-ligand. *Cell* 2002; **109**: 625–637.
31 Tagami K, Yujiri T, Takahashi T, Kizuki N, Tanaka Y, Mitani N *et al.* Increased serum levels of matrix metalloproteinase-9 in acute graft-versus-host disease after allogeneic haematopoietic stem cell transplantation. *Int J Hematol* 2009; **90**: 248–252.
32 Opdenakker G, Van den Steen PE, Van Damme J. Gelatinase B: a tuner and amplifier of immune functions. *Trends Immunol* 2001; **22**: 571–579.
33 Cauwe B, Van den Steen PE, Opdenakker G. The biochemical, biological, and pathological kaleidoscope of cell surface substrates processed by matrix metalloproteinases. *Crit Rev Biochem Mol Biol* 2007; **42**: 113–185.
34 Baker MB, Riley RL, Podack ER, Levy RB. Graft-versus-host-disease-associated lymphoid hypoplasia and B cell dysfunction is dependent upon donor T cell-mediated Fas-ligand function, but not perforin function. *Proc Natl Acad Sci USA* 1997; **94**: 1366–1371.
35 Panoskaltsis-Mortari A, Price A, Hermanson JR, Taras E, Lees C, Serody JS *et al. In vivo* imaging of graft-versus-host-disease in mice. *Blood* 2004; **103**: 3590–3598.
36 Wysocki CA, Panoskaltsis-Mortari A, Blazar BR, Serody JS. Leukocyte migration and graft-versus-host disease. *Blood* 2005; **105**: 4191–4199.
37 Hildebrandt GC, Duffner UA, Olkiewicz KM, Corrion LA, Willmarth NE, Williams DL *et al.* A critical role for CCR2/MCP-1 interactions in the development of idiopathic pneumonia syndrome after allogeneic bone marrow transplantation. *Blood* 2004; **103**: 2417–2426.
38 Tieu BC, Lee C, Sun H, Lejeune W, Recinos 3rd A, Ju X *et al.* An adventitial IL-6/MCP1 amplification loop accelerates macrophage-mediated vascular inflammation leading to aortic dissection in mice. *J Clin Invest* 2009; **119**: 3637–3651.

© 2015 Macmillan Publishers Limited